Vol. 44, No. 1 (2022) 97-112, DOI: 10.24874/ti.1054.02.21.06

Tribology in Industry

www.tribology.rs

RESEARCH

Effect of Varying Stand-off Distance on Tribological and Mechanical Properties of Plasma Sprayed Hydroxyapatite Coated Metallic Substrates

Sachin Solanke[a], Vivek Gaval[a,*], Ravi Thakur[b], Amit Pratap[a]

[a]*Institute of Chemical Technology, Mumbai 400019, India,*
[b]*Plasma Biotal India Pvt. Ltd., Pune 411021, India.*

Keywords:

Plasma sprayed hydroxyapatite coating
Stand-off distance
Microstructure
Sliding wear in Simulated Body Fluid
Mechanical properties

* Corresponding author:

Vivek Gaval

E-mail: vr.gaval@ictmumbai.edu.in

Received: 13 February 2021
Revised: 27 April 2021
Accepted: 2 June 2021

A B S T R A C T

Plasma spray technique is commonly used for the fabrication of hydroxyapatite (HA) coating for bio implants. Out of various process parameters in plasma spray technique, stand-off distance is one of the most important parameter which affects tribological and mechanical properties of the substrate. In the present work, HA powder was plasma sprayed onto Titanium grade 2 and Titanium grade 5 metallic substrates by varying standoff distance. Wear test was carried out to determine coefficient of friction and wear weight loss in the presence of simulated body fluid having a common pH of 7.25 similar to human blood plasma. The scanning electron microscopy and X-ray diffraction were used for characterization of microstructures and phase composition of coating respectively. Results have shown that HA coating obtained at 230 mm stand-off distance exhibits hardness and anti-wear characteristics as compared to coatings with stand-off distance of 180mm and 280 mm. This may be attributed to lower porosity and dense structure at a stand-off distance of 230 mm. The main wear mechanisms on the coating's wear track were found to be abrasive and adhesive.

1. INTRODUCTION

Hydroxyapatite (HA) has been clinically proven and acceptable bioceramic whose chemical composition is same as that of human bones. It has been extensively used for several years in the biomedical area for orthopedic load bearing implants. Generally medical metallic implants are coated with HA. The porous nature of HA and its lower fracture resistance cause rapid wear and, in some cases, earlier fracture of artificial implant bone, but chemical bonds with induced bone tissue are needed. The chemical bond between the metal prosthesis and the surrounding tissue is better when it is coated with HA [1]. However the most common causes of the orthopedic implant failure were found to be stress fatigue and wear. For artificial prosthetic applications of HA coatings, the coating lifetime is often limited by premature failure due to lower wear

resistance as earlier said. It is therefore highly important to understand the tribo-mechanical behavior of such bio-ceramic HA coatings because it is this property that governs the coating's intrinsic resistance against catastrophic failure. In this present research work, try to attempted an improve the wear resistance of HA coating forming by denser HA microstructure and to achieve a balance between the tribo-mechanical properties of the coatings by varying stand-off distance (SOD). Currently load bearing bioimplants such as knee and hip prosthesis undergo degradation after 12 - 16 years of use. The main reason of this degradation is wear failures as reported by various researchers [2,3]. Titanium alloys have been commonly used as orthopedic bioimplant prosthesis due to their high strength to weight ratio, very good corrosion resistance and biocompatibility. However, the used of titanium alloys are bounded because of their poor wear resistance and moderate surface hardness [4]. Metallic implant materials do not enhance tissue growth on their surface as a result poor fixation or loosening of the implant prosthesis which causes implant failure [5]. Khun et al. [6] observed better wear properties and friction coefficient for HA coating on titanium grade 5 plate formed by larger sized particles. Fu et al. [7] reported that fretting wear of HA-coated samples in dry testing conditions was worse than uncoated metallic samples. Buciumeanu et al. [8] reported that the wear behavior of HA-coated samples was influenced by applied load and lubricated conditions. However, very limited information is available on tribological properties of HA-coated titanium grade 2 (TIGR2) substrates using plasma spray technique with varying SOD in simulated body fluid. Therefore the present work dealt with this aspect.

One another major issue with metallic materials is release of metal ions in the body fluid environment when implanted in the living body which is dangerous and causes implant dissolution. More specifically, biologically this failure is known as the osteolysis [9]. For better tissue growth and longer functionality of implant, the releases of nano-metal ions in the vivo environment are required to prevented. These metallic surfaces were coated with HA bio-ceramic powder to solve problems [10]. Several surface modification techniques were investigated to improve properties of metallic alloys. Thermal coating process is found to be the most promising technique for coating metallic alloy bioimplant [11]. Out of this plasma spray technique which is suggested by the Food and Administration (FDA), USA, due to better HA coating properties as compared to other coating techniques [12]. The quality of bioimplant coating largely depends upon the selection of optimum process parameters in the plasma spray technique [13-15].

Spraying process parameters mostly influenced the mechanical and morphology properties of bioimplant coating [16]. User or operator can directly control or manage the primary parameters before or during the plasma process. It was reported that changing primary process parameters such as SOD, plasma power, and flow rate results in to variations of phase component, crystallinity, and microstructure of coatings [17]. The SOD has been identified as one of the important processing parameter which has a direct bearing on microstructures and properties of HA coatings. It was reported that amorphicity of plasma coating increased and relative crystallinity decreased with the SOD increasing [18,19]. With the optimum SOD, the porosity of coating reduces due to an increase in the degree of molten lamellae in thermal fabrication methods [20]. Earlier tribological behavior of the HA coatings developed by micro plasma sprayed technique on the Ti6Al4V metal samples studied at low load and author reported 0.8 average value of friction coefficient (COF) [21]. Tribological studies of different bioimplant materials for orthopedic application were carried out on bare substrates samples. It was reported that wear loss and COF did not change noticeably with increasing the wear parameter including load and velocity [22]. The scope of the problem and the objective of the present research have been formulated after detailed literature review.

Although a lot of research has been undertaken in this area, detailed investigations are required to be carried out to achieve quality HA-coated TIGR2 material bio-implants. The objective of this study was to understand the relationship between in vitro wear behavior, microstructural properties of the coating, and the SOD. This research also provides some important guidelines pertaining to operational conditions for the fabrication of high-quality HA coatings for bio-implants.

2. MATERIALS AND EXPERIMENTAL PROCEDURES

Photographs of an uncoated specimen, HA-coated specimen, and a worn-out specimen are shown in figure 1(a), (b) and (c).

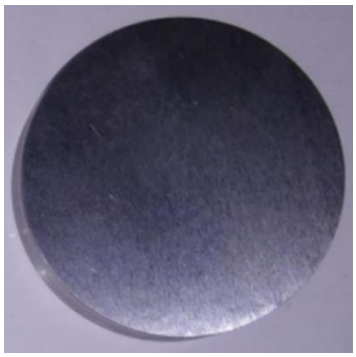

(a)

(b)

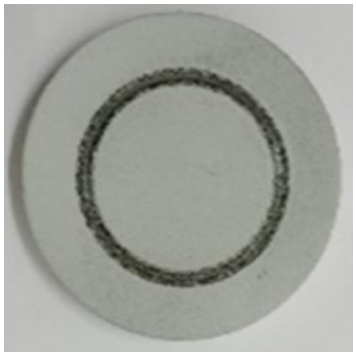

(c)

Fig. 1. (a) Uncoated metallic samples, (b) HA-coated sample, (c) Wearout sample after tribo-test.

2.1 Preparation of substrate samples

The metal substrates such as Titanium grade 5 (TIGR5), TIGR2 were purchased from the Belmount Industrial Solutions, Mumbai, India. The substrates were obtained in solid form. Laser technology was used to prepare samples having 40 mm dia. and 4 mm thick required for in vitro wear test. Densities of TIGR5 and TIGR2 are 4.43 g/cc, 4.52 g/cc respectively [23,24]. The metallic substrates were polished and subsequently cleaned ultrasonically in acetone followed by drying in an oven at 75^0 C for 30 minutes to remove any traces of unwanted material and debris embedded on the sample surface during the preparation of samples using laser technology. The sample preparation was as per ASTM G99-95a. The materials used for load bearing implants such as hip and knee prosthesis must be strong under fatigue loading and biocompatible. Now day's titanium and its alloys are widely used as orthopedic implants [25].

2.2 Hydroxyapatite powder

Sintered and granulated HA powder with a good flow ability was obtained from Plasma Biotal India and used as feedstock. Having particle size between 30-60 µm, Crystallinity > 95%, Phase purity > 95% and Ca/P ratio- 1.67. Captal® 60 sintered HA is a medical-grade, synthetic, high-purity, highly crystalline bioresorbable bone substitute material designed to closely mimic the properties and composition of natural bone. Average HA powder particle size of 41 µm was used for coating TIGR5 and TIGR2 metallic substrate samples. HA meets the requirements of the ISO 13779-6 international standard [26]. The physical properties of plasma HA powder are as shown in table 1.

Table 1. Physical properties of plasma biotal India ltd. HA powder.

Morphology	Spherical
Colour	Pale Blue
Bulk Density	0.55 - 0.90 g/cc
Tapped Density	0.75 - 1.20 g/cc
Particle absorption index	0.005
Particle Refractive index	1.670

From the laser diffraction method, the average size of the sinter-granulated HA powder was observed to be ~41 µm. It is reported in the published research that the moderate size (30–55µm) particles have produced a much denser lamellar coating than larger size particles which has resulted in better mechanical properties of coating [27]. So in this study, HA powder with average particle size of 41 µm was used to produce denser and good quality coatings [28]. The flow rate of the HA powder was measured as ~0.5 gm/sec using Hall - Flowmeter. The particle size distribution of the HA powder is as shown in figure 2.

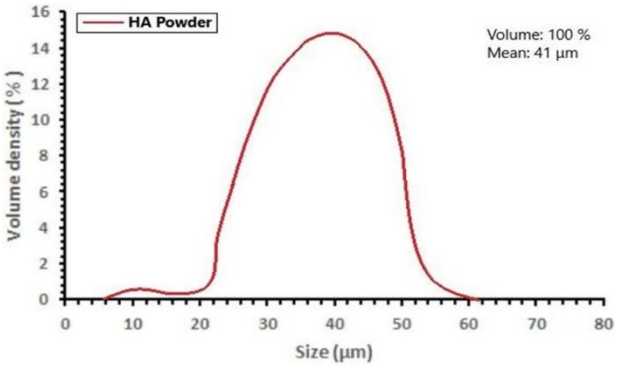

Fig. 2. Particle size analysis of sinter-granulated HA powder.

The SEM images and corresponding XRD spectra of the sintered HA powder are shown in figure 3(a), 3(b) and 4 respectively. The XRD pattern of HA bioceramic powder showed the major existence of HA peaks. It observed there is a good match with the standard (JCPDS file no. 09-0432) both in terms of intensity and position of the HA peaks.

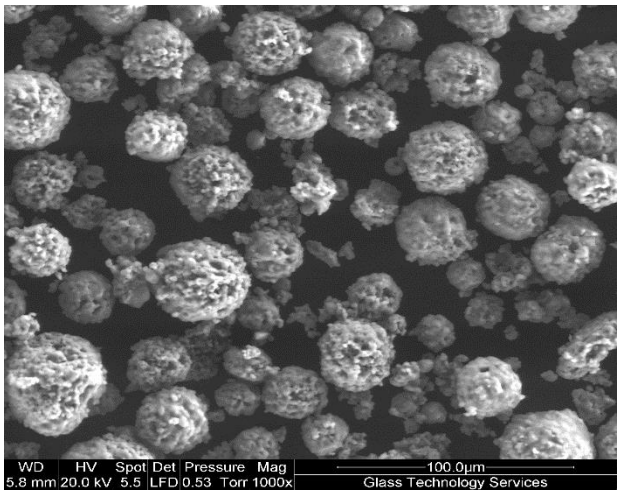

(a)

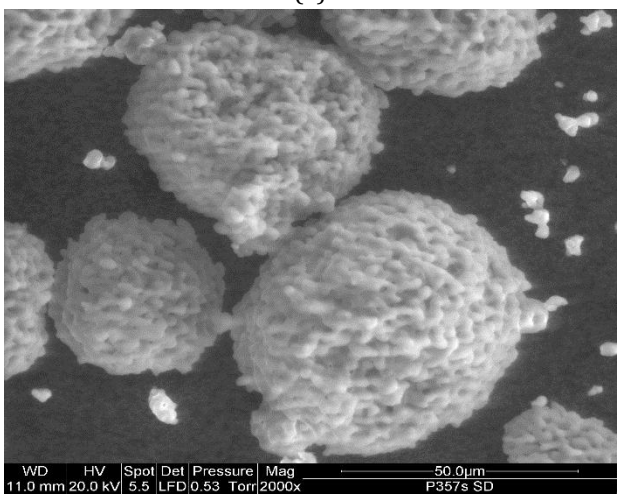

(b)

Fig. 3. (a) SEM micrograph of HA powder, (b) SEM micrograph of HA powder.

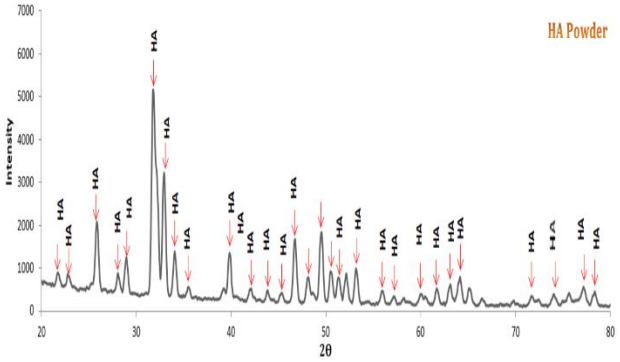

Fig. 4. XRD image of HA powder.

2.3 Coating preparation

The HA coating on TIGR5 and TIGR2 was fabricated by using plasma spray technique at Plasma Biotal India Ltd., Pune, India. Prior to depositing HA coating, the metallic samples were grit blasted at a blasting pressure of 4- 5 bar so as to improve the bond strength between the HA coating and the metallic substrate. Pure white alumina (Al_2O_3- 200 to 250 µm) at high velocity was used to get the desired surface roughness between 2.5 to 3.5 µm. Grit blasting is most commonly used standard surface roughening technique for plasma spraying applications. Metallic substrate surface roughness significantly affects adhesive strength of plasma sprayed HA coatings. Some impurities or grease on the surface of the metallic substrate will greatly reduce the coating bond strength and results in delamination or cracking. The ultrasonic cleaning (Ultrasonic cleaning system, Model: Microclean-103, 120 W, 3 liter) was carried out for 5 minutes (ISO 19227:2018) to remove alumina grit particles which got embedded on metallic substrate during blasting [29]. The commercials Sulzer Metco 9MB-Dual Plasma Spray Gun (80 kW, 9MBM machine-mount, UniCoatPro Plasma, 9MC, 9MCE) was used to develop HA coatings. Table 2 presents the plasma spray technique process parameters used for coating of HA powder on metallic substrates. In this study, Argon was used as both the primary and secondary gas to prevent oxidation. Secondary gas creates an inert shroud over the particles that shields against the oxidation of hydroxyapatite.

The typical HA coating thickness observed was around 146 ± 20 µm on TIGR5 and TIGR2 metallic substrate samples as evident from SEM micrograph. For the measurement of plasma sprayed HA coating thickness, 5 measurements were taken at roughly 100 µm intervals. Figure 5 depicts the cross-sectional microstructures of the plasma sprayed HA coating.

Table 2. Plasma process parameters to develop HA coatings.

Sr. No.	Process Parameters	Value with unit
1	Plasma power	25- 28 kW
2	Primary gas	Argon
3	Secondary gas	Argon
4	Flow rate	08 -10 g/min
5	Stand-off distance (SOD)	180 mm, 230 mm, 280 mm
6	Traverse Velocity	38 - 46 mm/s

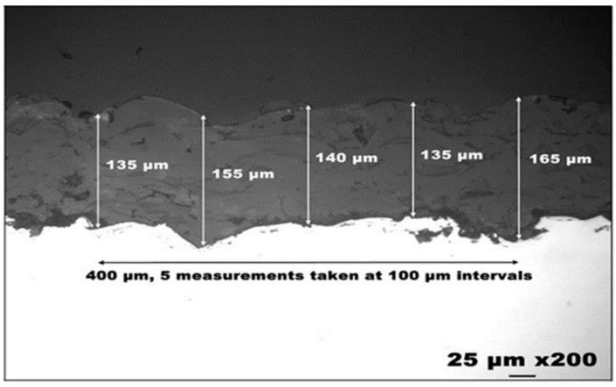

Fig. 5. Cross-section photomicrograph represents coating thickness of HA coating.

2.4 Microstructure characterization

The HA sprayed coatings and worn-out surfaces of HA coated samples were inspected under FE-SEM (ZEISS- Gemini, Cambridge CB 1 3JS, United Kingdom) for microstructural characterization of the HA coatings at MMMF lab, IIT Bombay. The percentage open porosity of the HA coatings was analyzed by using Image J software (Java-based, Version 1.52 v, National Institutes of Health and the Laboratory for Optical and Computational Instrumentation). The reported values are the average of five measurements at distinct locations of HA coating. EMPYREAN diffractometer system was used to perform XRD analysis and to obtain the phase composition in the plasma HA powder and developed plasma HA coatings. During X-ray diffraction the 2θ value was kept between 20° to 80° with 0.02° step size. EDS analysis of HA coated samples was performed at different locations to confirm the weight percentage of elements in the coating.

2.5 Mechanical properties evaluation

Microhardness of the coating: Nanoindentation technique was used to evaluate two local mechanical properties such as nano-hardness (H) and elastic modulus (E). Nanoindentation test was carried out at industrial research and consultancy center, IITB (Hysitron Inc Minneapolis USA, TI-900). H is measured as the ratio of maximum applied load to the area of contact and reduced E is from the load versus depth of penetration plots using the well-established Oliver and Pharr (O-P) method. The load was kept constant at 10 mN. Ten indents were made for each coated sample at different location on the sample. Ten repeat experiments were performed on each HA coated samples and average value of ten tests was considered. For the nanoindentation experiments Berkovich indenter was used with 65.3^0 semi-apex angle and small tip radius around ~200 nm. The nanoindentation experiments were carried out using DIN 50359-1 standard.

Bonding strength measurement: The bonding strength of the HA coating was measured using ASTM- C633 standard .This was carried out at plasma Biotal India Pvt. Ltd., Pune, India (5500R, Instron, USA). The HA coated sample was mounted between the two cylindrical jigs made of stainless steel using FM 1000 polyamide-epoxy resin film. HA coated metallic substrates were acted upon by tensile load in the normal direction till the commencement of fracture at HA - metal substrate interface. The applied tensile load was then slowly increased from the failure occurs. The adhesive strength is then computed using ratio of load to area at failure. The average value of adhesive strength was considered on the basis of three measurements for each sample. In most of the cases the fracture was observed at the interface between the metal samples and the coated HA layer.

2.6 Tribological tests

Ball on disc machine (TR-30LE CHHM-800, DUCOM Instruments, Bengaluru, India) was used to conduct unidirectional wet sliding wear tests at room temperature under simulated body fluid (SBF). SBF is prepared with the help of Kokubo's recipe [30], whose Ion concentrations is exactly equal to human blood plasma pH between 7.20 to 7.40. Steel balls indenter of 10 mm diameter which having hardness value 62 (HRC) were used as a counter surface (indenter). The balls are specially made as per our requirement and purchased from Ducom instruments, Bengaluru, India. Prior to test the samples were cleaned with

ethanol in order to remove the dust on HA coated surface of samples. In ball on disc machine, the flat disk is rotated against the stationary ball at a specified load. Flat disk is made of AISI 52100 steel.The wear between the samples and ball was noted by LVDT sensor which was mounted on the machine. Wear ball on disk machine connected with a computer (ACER VERITON M200-H81 DESKTOP, PCI-E-6321 NI Card, DUCOM, Benguluru, India). The PC is loaded with WINDUCOM 2010 software for displaying the results in graphical form. The wear experiments were performed using ASTM G99 standard. During the test the wear loss and COF values were recorded and analyzed. Selection of wear parameters was based on the similar conditions of wear to which the femoral ball head is subjected inside the acetabular cup. Generally during walking the stress produced in a hip prosthesis is in the range of 0.7 to 4 MPa [31]. HA coated hip prosthesis is expected to sustain frictional forces for a minimum of 18 to 25 years [32]. Since it is not feasible to carry out wear studies for a period of 18 to 25 years, the high value of applied normal load in the order of 10 N is maintained during wear testing. For determining the average wear weight loss of HA-coated samples, five repeat experiments were carried out and an average value of five measurements was considered. Table 3 presents general characteristics of coating and experimental parameter related to wear test.

Table 3. General characteristics of coating and experimental parameter related to wear test.

Disc materials	Plasma coated
Coating thickness	146 ± 10 μm
Coated disc dia.	Φ 40 mm
Ball dimension (indenter) for wear test	Φ 10 mm
Normal load	10 N
Sliding velocity	0.1 m/s

3. EXPERIMENTAL RESULTS AND DISCUSSION

3.1 Microstructure and phase constitution

Figure 6 shows the X-ray diffractometer (XRD) pattern of a typical plasma sprayed HA coating. The pattern was thoroughly indexed as per ICSD standard and shows the crystalline phases of HA as expected. Figure 7(a), 7(b) and 7(c) shows the typical X-ray spectroscopy (EDS) spectrum of plasma sprayed HA coatings. It could be evidently observed that the signatures of Ca, P, and O are present as they are major constitutes of HA coatings. The EDS data (Table 4) shows that the HA coatings developed by plasma spraying had stoichiometric Ca/P of near to 1.67 that bears the signature of the pure HA phase formation. The presence of other elements may be due to the adhesive disc used to fix the sample holder.

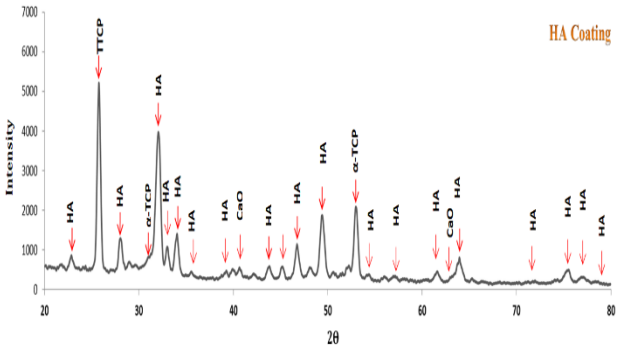

Fig. 6. XRD pattern of a plasma sprayed HA coating.

Table 4. Values of Ca/P in different spots of HA coatings.

Element	Fig 5 (a)	Fig 5 (b)	Fig 5 (c)
Ca	34.6	39.6	46.7
P	20.4	23.6	27.9
Ca/P	1.69	1.69	1.67

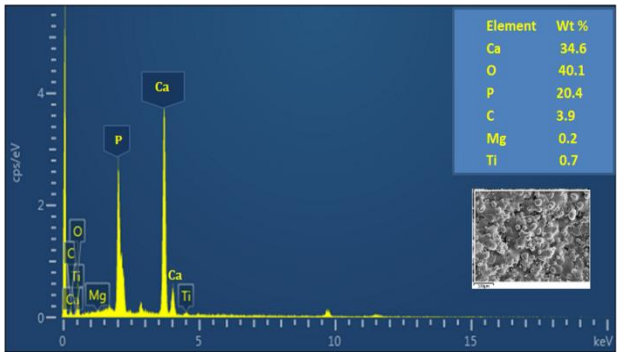

(a)

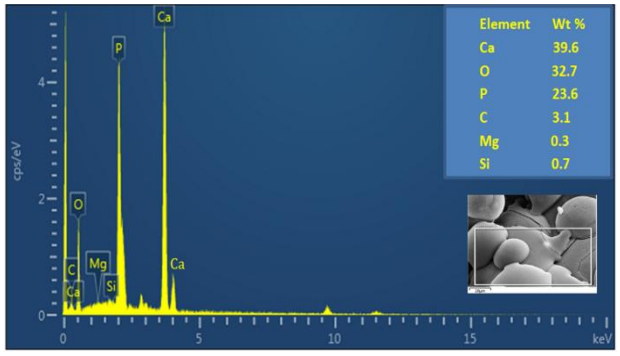

(b)

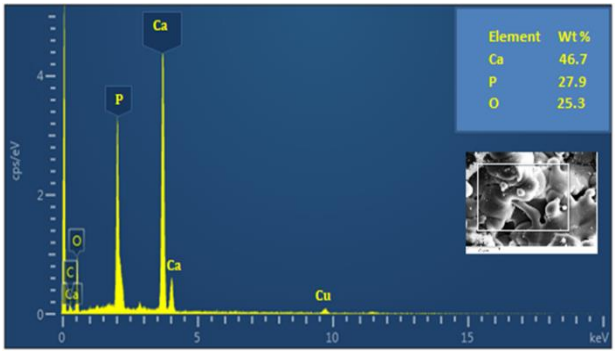

(c)

Fig. 7. (a) EDS spectra of HA coatings in different spot, (b) EDS spectra of HA coatings in different spot, (c) EDS spectra of HA coatings in different spot.

Figure (8-13) shows the plan-sectional microstructures of the plasma-sprayed HA coatings developed at a SOD of 180, 230 mm and 280 mm, respectively. Coating with lower (180 mm) and higher (280 mm) SOD comprised of irregular splats shaped, nano intersplat crack, unmelted semi-melted powder particle, as well as a significant amount of nano, meso, and micro porosities. However, at a SOD of 230 mm, SEM images show denser microstructure and less porosity. This may be because of the filling of voids between neighbouring splats by spherodized and melted HA particles.

The microstructure in figure 8 (coating at 180 mm SOD) depicts many pores and unmelted particles. Such particles are not fully well integrated into the coating. Whereas figure 9 and 13 (coating at 230 mm SOD) demonstrates a structure with flatten splats and fewer voids, which is indicative of improved packing of the layer, reduces the inter-splat region and particle melting giving rise to a typical lamellar structure with splat bonding.

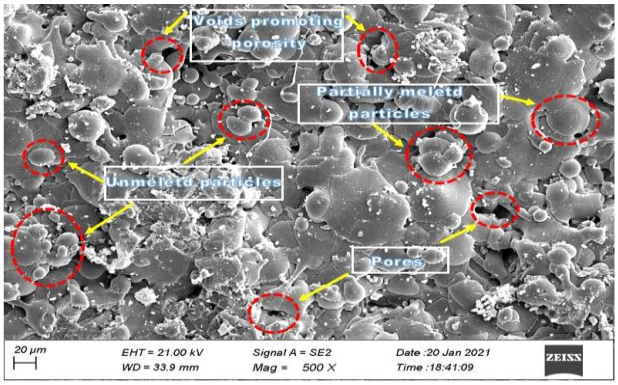

Fig. 8. Micrograph of plasma coating at TIGR5- 180 mm SOD.

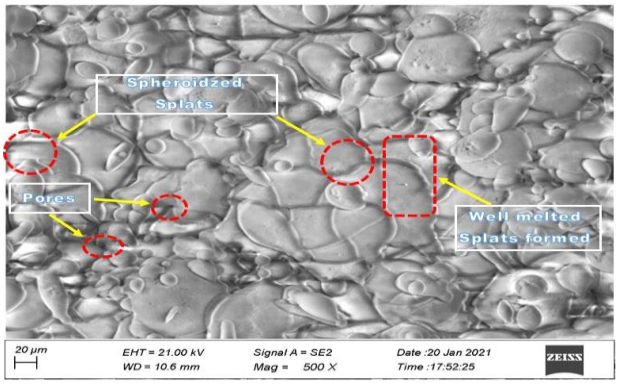

Fig. 9. Micrograph of plasma coating at TIGR5- 230 mm SOD.

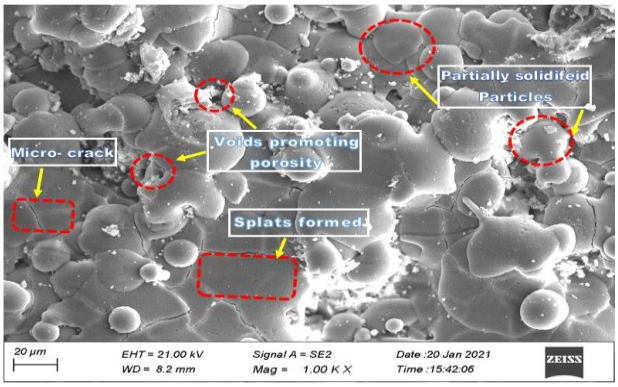

Fig. 10. Micrographs of plasma coatings at TIGR5- 280 mm SOD.

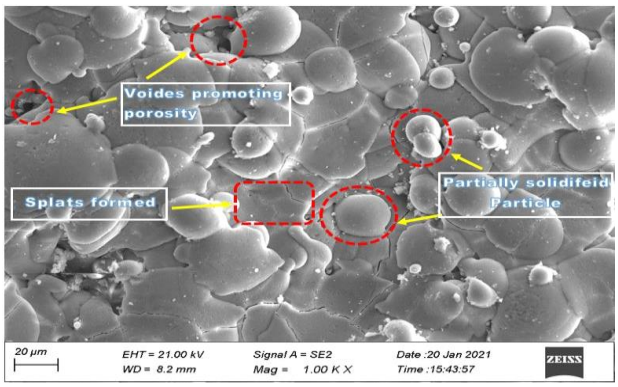

Fig. 11. Micrograph of plasma coating at TIGR2- 280 mm SOD.

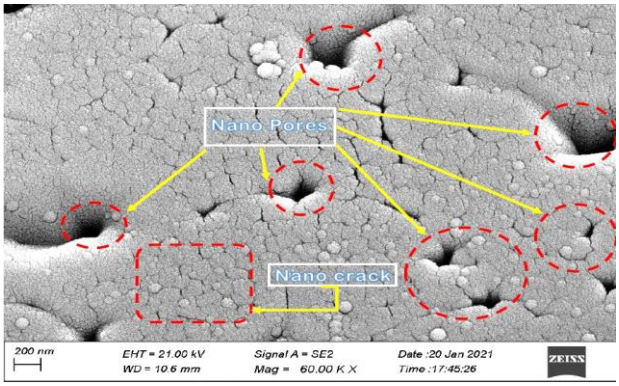

Fig. 12. Micrograph of plasma coating at TIGR5- 180 mm SOD.

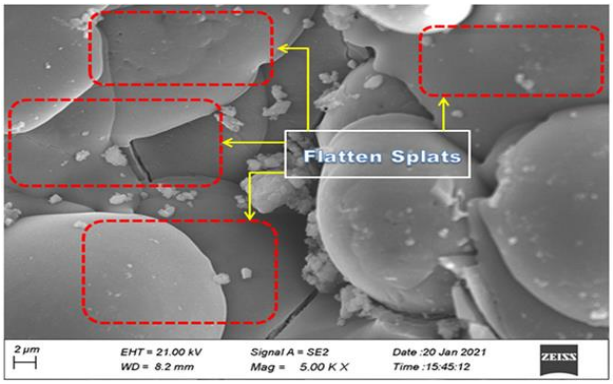

Fig. 13. Micrograph of plasma coating at TIGR2- 230 mm SOD.

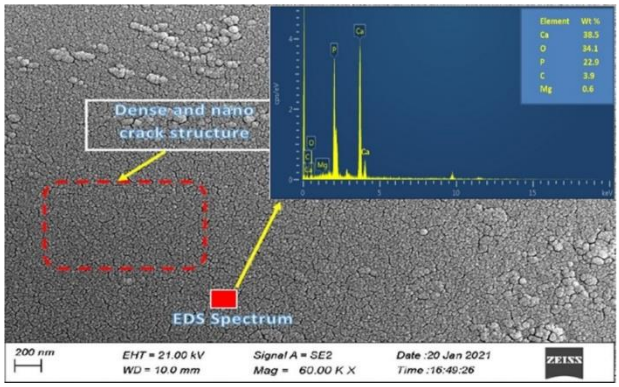

Fig. 14. Micrograph and EDS Spectra at TIGR2- 230 mm SOD.

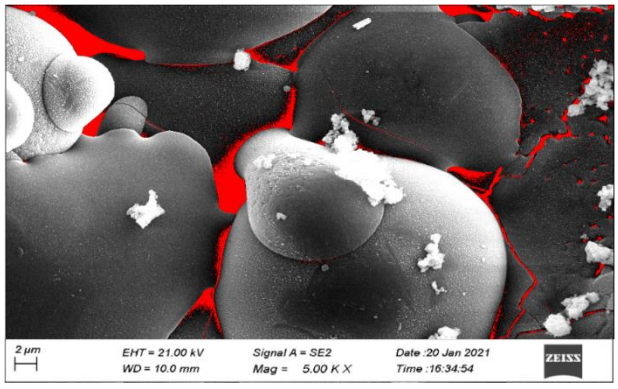

Fig. 15. Micrograph showing porosity in Image J software at TIGR2- 280 mm SOD.

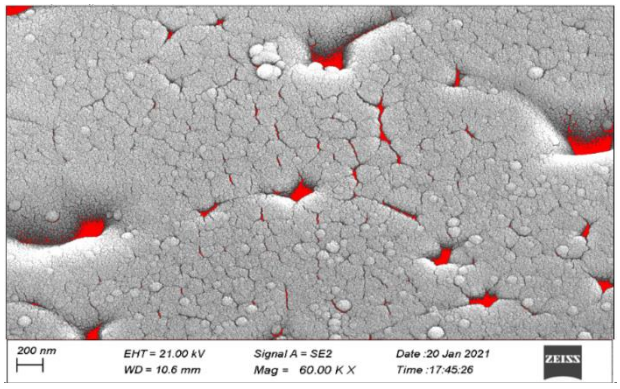

Fig. 16. Micrograph showing porosity in Image J software at TIGR5- 180 mm SOD.

3.2 Mechanical properties of the coatings

For the nano-indentation test, the maximum depth of penetration was kept well below 10% of the HA coating thickness so as to avoid influence of mechanical properties of substrate on the measured data. As the microstructure of the HA coating was observed to be heterogeneous and porous, at least 10 indents were made at randomly chosen different locations on the coated sample surface so as to obtain statistically valid and reliable data. There is an inverse relationship between hardness and porosity, i.e., as the porosity reduces the hardness increases. With the increase in porosity of plasma sprayed HA coating, mechanical properties are severely affected. Porosity is one of the most significant factor in plasma- sprayed coatings [33]. Figure 17 and 18 shows the variation in the porosity and adhesive strength values for plasma sprayed HA coatings measured at various SODs for TIGR5 and TIGR2.

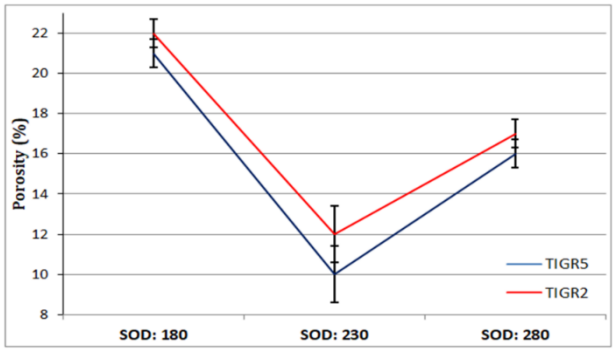

Fig. 17. Porosity versus varying SOD.

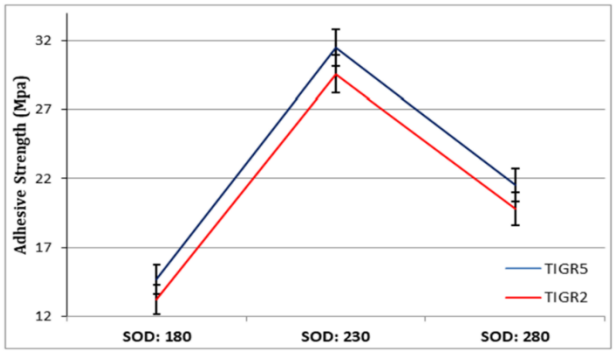

Fig. 18. Adhesive strength versus varying SOD.

The computed bonding strength value between the HA coated layer and metal substrates observed in the range of 14.7 to 31.5 MPa for TIGR5 and 13.2 to 30.6 MPa for TIGR2 material. These range of values indicates formation of strong bond between HA coating layer and metal

substrates. As per the industrial standard the mean coating adhesion strength shall be greater than 15 MPa (ISO 13779-2, ISO 13779-4) [34,35]. Figure 19 and 20 shows the variation of H and E for plasma sprayed HA coatings at various SODs for TIGR5 and TIGR2 substrates.

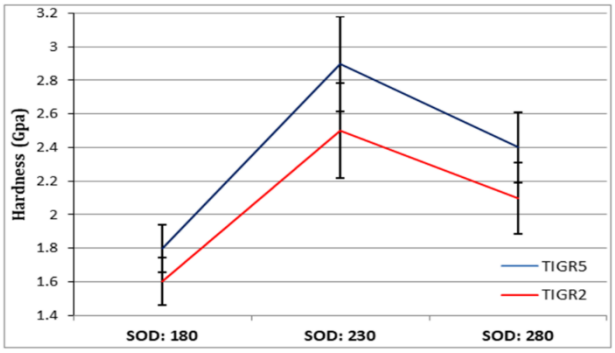

Fig. 19. Hardness versus varying SOD.

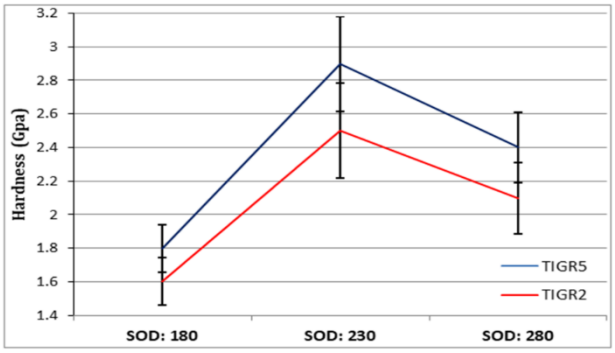

Fig. 20. Elastic modulus versus varying SOD.

In the present work, the HA coating at 180 mm SOD showed minimum elastic recovery and nano hardness by virtue of higher porosity evident from SEM resulting in a lesser value of E. The porosity values are found to be maximum for the HA coating developed at the shortest SOD of 180 mm. This happened possibly due to knockback or rebound action of un-melted or partially melted particles/splats impinging on to the substrate samples as the distance of exit nozzle and the substrate is very short [19,20]. Unmelted splats retaining a non-flattened core results in the formation of micro-pores structure. Also the particles are exposed to flame for less time resulting in less heat work on the HA. Even if the particles are melted there is a possibility of higher viscosity leading to poorer splats.

At 230 mm SOD properties such as adhesive strength of the coating, hardness of the coating, and elastic modulus are found to be better as compared to a SOD of 180 mm and 280 mm. This may be due to lower porosity and dense microstructure observed at a SOD of 230 mm. The 50% reduction in porosity at 230 mm SOD may be attributed to appropriate in-flight particle temperature and velocity carried by the HA powder when exposed to plasma flame which may increase the degree of spheroidzed and molten lamellae which results in melted lamellae well stack together on the substrates [36]. On the other hand, porosity is increased at longer 280 mm SOD from 230 mm to 280 mm, some HA particles might be unable to reach the end of the sample due to the journey of long-distance and reduction in velocity of melted particles. The particles could solidify partially before reaching to the substrate samples due to the long distance and the drop in plume temperature which in turn produces splats which are randomly deposited leading to form further micro-pores structure and as observed and also reported in published research [37]. The hardness and elastic modulus values for different HA-coated samples at various SODs are as shown in table 5.

Table 5. Microstructural properties of plasma-sprayed HA coatings developed at different SOD: 180, 230 and 280 mm.

Plasma sprayed HA coatings	Adhesive strength of coating (MPa)		Porosity (%) of coating		Hardness of coating (GPa)		Elastic modulus of coating (GPa)	
	TIGR5	TIGR2	TIGR5	TIGR2	TIGR5	TIGR2	TIGR5	TIGR2
SOD: 180 mm	14.7±0.47	13.2±0.42	21±2.17	22±2.21	1.8±0.75	1.6±0.78	70±1.23	68±1.31
SOD: 230 mm	31.5±0.31	30.6±0.35	10±2.06	12±2.01	2.9±0.70	2.5±0.68	86±1.07	83±1.02
SOD: 280 mm	21.5±0.40	19.8±0.38	16±2.25	17±2.30	2.4±0.85	2.1±0.91	75±1.12	71±1.15

3.3 Friction and wear characteristics

To measure weight loss of materials, the weight of HA coated substrate samples (before and after test) was recorded by Electronic Weighing machine (Contech Instruments Ltd., Navi Mumbai, India). Average weight loss of the HA coated substrate materials in grams is as shown in table 6. Measurement uncertainty @ 95% confidence level was observed ± 0.0001 gm.

Table 6. Wear weight loss (Gram)

Measurement Number	Wear weight loss (Gram)					
	TIGR5			TIGR2		
	SOD-180	SOD-230	SOD-280	SOD-180	SOD-230	SOD-280
1	0.0076	0.0060	0.0069	0.0083	0.0062	0.0074
2	0.0079	0.0057	0.0067	0.0081	0.0064	0.0072
3	0.0078	0.0058	0.0070	0.008	0.0062	0.0071
4	0.0079	0.0061	0.0066	0.0081	0.0063	0.0073
5	0.0078	0.0057	0.0068	0.0083	0.0065	0.0071
Minimum	0.0076	0.0057	0.0066	0.0080	0.0062	0.0071
Mean	**0.0078**	**0.0059**	**0.0068**	**0.0081**	**0.0063**	**0.0072**
Maximum	0.0079	0.0061	0.007	0.0083	0.0065	0.0074
S.D. (σ)	0.00012	0.00018	0.00015	0.00013	0.00013	0.00013
RSD (%)	1.57	3.10	2.33	1.64	2.07	1.81
Confidence Interval	0.0078 ± 0.00010	0.00586 ± 0.00015	0.0068 ± 0.00013	0.00816 ± 0.00011	0.0063 ± 0.00011	0.0072 ± 0.00011

Table 7. Average value of COF

TIGR5			TIGR2		
SOD-180	SOD-230	SOD-280	SOD-180	SOD-230	SOD-280
0.81	0.48	0.65	0.88	0.57	0.69

The plasma-sprayed coating shows minimum wear loss and minimum COF at 230 mm SOD which is attributed to the dense and nonporous microstructure of coating resulting in higher wear resistance. The SEM images for 180 mm SOD for both the substrates reveal the presence of semi-molten HA powder particles and porous microstructure to a large extent resulting in more wear weight loss. The average wear weight loss and coefficient of friction (COF) of the HA coatings at 280 mm SOD was observed to be slightly higher as compared to a 230 mm SOD. This may be due to lower hardness and the presence of semi-molten HA powder particles in HA coating. The wear track generated for HA-coated samples for TIGR5 and TIGR2 at 280 mm SOD was observed to be more profound and broader with significant wear loss as compared to at 230 mm SOD.

Higher wear rate showed the short life of an orthopedic component [38]. Generally wear debris from the coatings undergo biodegradation completely due to macrophages and neutrophils phagocytes. If it does not undergo biodegradation then it will be cleared out from renal excretion route very quickly by the immune system of body. Retention of these wear debris causes infection and toxicity in any organ [39,40-42]. The tribological properties of plasma sprayed HA coated TIGR5 substrate are found to be marginally better as compared to HA coat TIGR2 substrate. This may be due to mechanical anchorage, good atomic coherence property and physical chemical interaction as reported in literature [5,43,44]. Lowered atomic coherence equates to weakened chemical bond of coating. Figure 23 shows the average wear loss for plasma sprayed HA coated TIGR5 and TIGR2 substrate against bearing steel ball. Wear loss which is mainly due to plastic deformation of HA coatings.

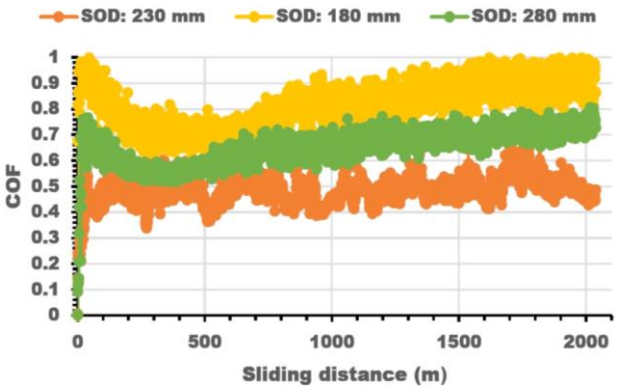

Fig. 21. Coefficient of friction as a function of sliding distance for TIGR5- HA coated samples at different SOD: 180 mm, 230 mm and 280 mm in wet condition.

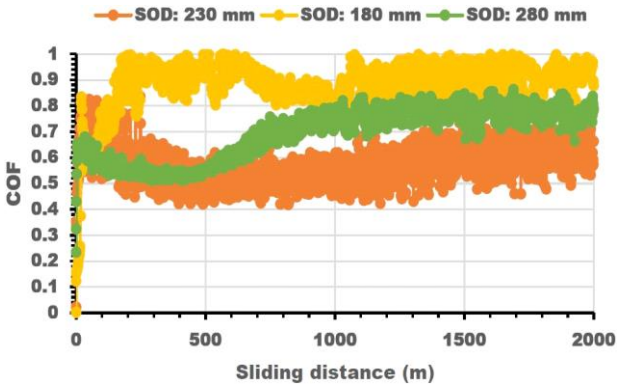

Fig. 22. Coefficient of friction as a function of sliding distance for TIGR2- HA coated samples at different SOD: 180 mm, 230 mm and 280 mm in wet condition.

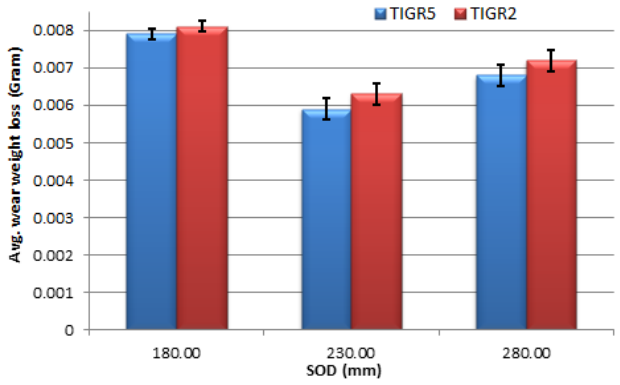

Fig. 23. Average wear weight loss for TIGR5- HA and TIGR2- HA coated samples at different SOD: 180 mm, 230 mm and 280 mm in wet condition.

The average COF values for the present HA-coated substrates at different SOD were found to be well within the typical range (e. g. 0.5 to 0.9) as reported by researchers [7,45,46].

3.4 Worn surface morphology

The wear mechanism is significantly influenced by adhesion and abrasion with brittle cracking, brittle rupture, abrasive grooving, and spalling pits. This may be due to severe plastic deformation (plasticization), plowing, and grain fragmentation of coatings. SEM images of worn-out surfaces clearly depict spalling, brittle cracking /rupturing. Figure 26 clearly shows the comparison between HA-coated surface before tribo-testing and worn-out surface after the tribo-testing. The formation of dense microstructure at 230 mm SOD resulted in less amount of brittle cracking and brittle fracture against the hard steel ball indenter. Because of this wear resistance characteristic of the HA coatings have shown improvement. The progression of matrix abrasion was observed to be comparatively slower in plasma-sprayed HA coatings at 230 mm SOD. The wear tracks generated for HA-coated samples for TIGR5 and TIGR2 at 180 mm SOD were observed to be more profound and broader with significant wear loss.

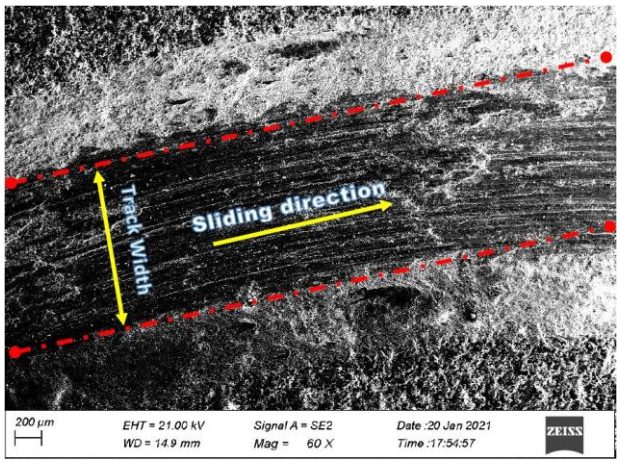

Fig. 24. Scanning electron micrographs of worn-out plasma coatings after tribo-test at TIGR5- 180 mm SOD.

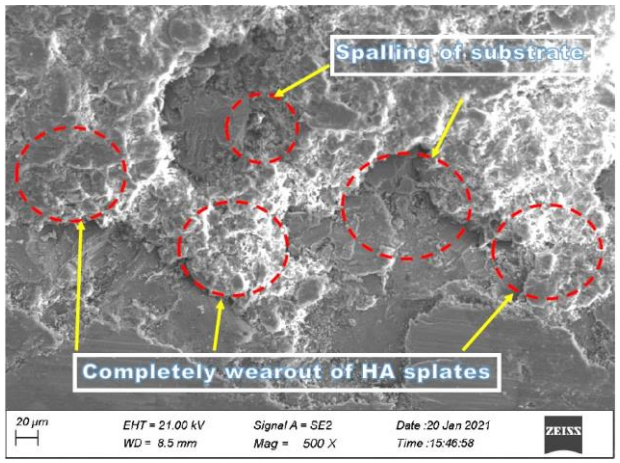

Fig. 25. Scanning electron micrographs of worn-out plasma coatings after tribo-test at TIGR2- 180 mm SOD.

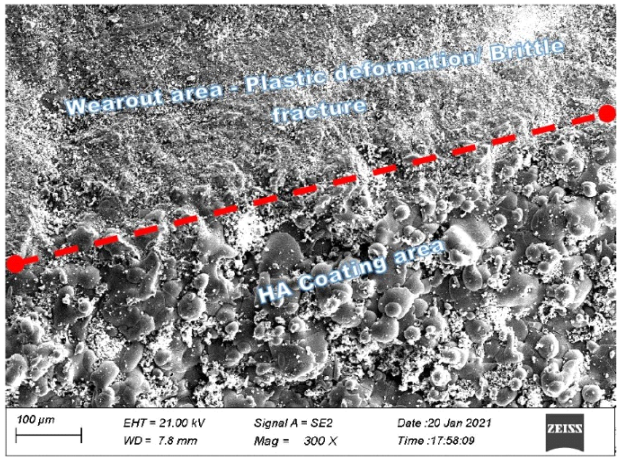

Fig.26. Scanning electron micrographs of worn-out plasma coatings after tribo-test at TIGR5- 230 mm SOD.

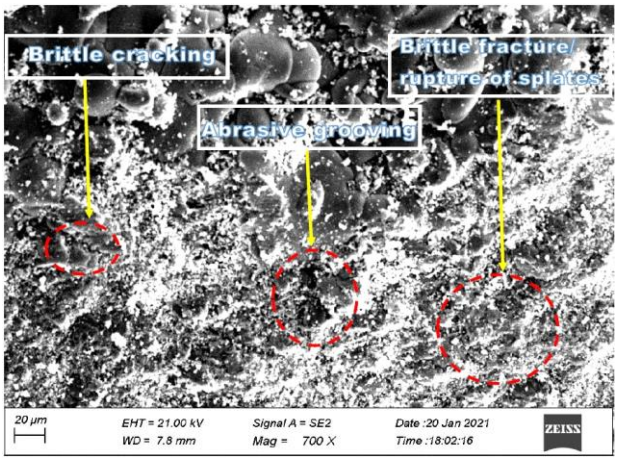

Fig. 27. Scanning electron micrographs of worn-out plasma coatings after tribo-test at TIGR5- 280 mm SOD.

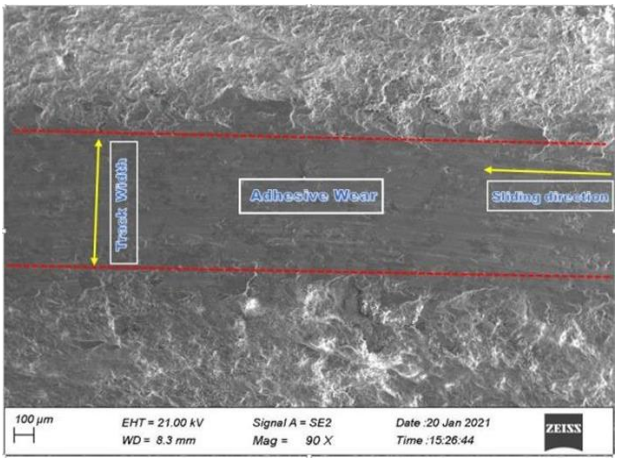

Fig. 28. Scanning electron micrographs of worn-out plasma coatings after tribo-test at TIGR2- 230 mm SOD.

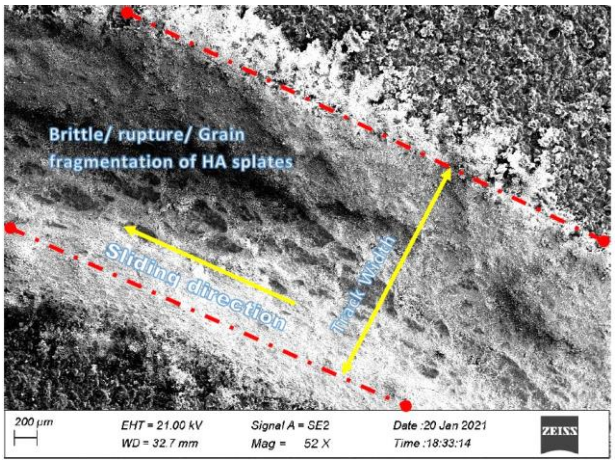

Fig. 29. Scanning electron micrographs of worn-out plasma coatings after tribo-test at TIGR2- 280 mm SOD.

Mostly two-body severe abrasive wear was observed due to sliding rotation of hard steel ball against the brittle HA coating samples. At a SOD of 180 mm, complete wear of HA splats and spalling pits in the bare substrate was observed. This may be due to higher contact stress between relatively hard steel ball and HA coating as shown in figure 25. The brittle cracking and rupturing across the HA splats is clearly seen on the coated surface due to the formation and existence of large volume pores in the plasma sprayed HA coatings at 280 mm SOD. Under the wet sliding condition, the wear debris trapped between the steel ball indenter and the HA coating surface acts as a third body abrasion. This wear phenomenon has contributed to the propagation of abrasion grooves. Figure 24 shows the wear streaks on the wear track of HA-coated samples indicating the existence of wear debris possibly due to the removal of the asperities by plasticization and shearing. This wear mechanism is found to be more severe in the plasma sprayed HA-coated substrates at a SOD of 180 mm and 280 mm. Figure 29 shows the presence of macro brittle crack alongside with surface pores in the HA coating at higher magnification. This macro brittle crack on reaching the critical size results in the formation of wear debris in the form of fragments. The wear mechanism observed in this present research work is very much similar to the wear mechanism as reported in research studies that have been carried on HA coatings formed by different thermal processes [47-49].

The adhesive strength of HA-coated samples at optimum SOD in the present work is found to be better as compared to samples fabricated by other methods as reported in the published research [50, 51]. On comparing with samples fabricated by the plasma spraying method in the reported literature [21,52], the coated samples in the present work exhibit better wear resistance and micro-hardness. However, the direct comparison of experimental results in this study with the published research seems to be difficult because of the different HA coating deposition methods and process parameters used in published research.

Some pores in the prosthesis encourage tissue to grow in and anchor the prosthesis to the surrounding bone, preventing implant loosening. But, a high porous coating structure is likely to have poor substrate adhesion and tribo-mechanical ability, In that the coating will delaminate and release extremely undesirable debris, impeding osseointegration by eliciting unacceptable tissue responses Furthermore,

excessive body fluid penetration in the coating can result in the dissolution of the coating material in the interface area, resulting in adhesive strength weakening [18,41,53,54]. Due to the shorter residence time in the plasma flame at 180 mm SOD, HA powder particles melt at a very low rate. As a result, particle spreading is reduced, resulting in a higher number of pores in the coating. Whereas HA coating at longer SOD 280 mm, longer residence time in the plasma flame results in more heat work on the powder and greater quenching amount upon 'splat' due to additional work these leads to the formation of the weak coating. Optimal pores with flatten splats, denser structure, and fewer voids were observed at 230 mm SOD as compared to other SOD. Micro-indentation and the tribological test result showed that HA coating at 230 mm SOD had better hardness and wear resistance. Therefore, HA coating fabricated at 230 mm SOD can be considered as better rather than at 180 mm and 280 mm SOD.

4. CONCLUSION

At 230 mm SOD, the Plasma sprayed HA coating has low porosity, denser microstructure, and higher hardness. The HA-coated TIGR5 samples exhibited lower wear loss and lower coefficient of friction as compared to HA-coated TIGR2 samples. Hence SOD of 230 mm is considered to be optimum with existing values of other parameters for quality plasma sprayed HA-coated titanium substrates. At 180 mm SOD, scanning electron micrograph revealed profound and broader wear track generated on both substrates because of porous microstructure and lower hardness. This is attributed to the rebound action of unmelted or partially melted HA powder particles impinging on substrates. At 280 mm SOD, the tribological and mechanical properties of plasma sprayed HA-coated substrates are better as compared to 180 mm SOD but inferior as compared to 230 mm SOD. This may be due to partial solidification of particles before reaching substrates at 280 mm SOD. So it is concluded that tribological and mechanical properties of plasma sprayed HA-coated substrates are greatly affected by changing SOD and are found to be better at 230 mm SOD. The microhardness test, tribo-test, and scanning electron micrographs at various SOD support the increase or decrease in tribological and mechanical properties.

Acknowledgements:

The authors sincerely thank to Plasma Biotal India Pvt. Ltd., Pune, India for providing the HA coatings and testing facility and support. The authors are thankful to MMMF Lab, IIT-B, Mumbai, INDIA for providing the experimental facilities like XRD, SEM, EDS etc. The authors grateful to general engineering department, ICT, Mumbai, INDIA for availing the research support and direction to carried out present research.

REFERENCES

[1] S.P. Khanal, H. Mahfuz, A.J. Rondinone, T. Leventouri, *Improvement of the fracture toughness of hydroxyapatite (HAp) by incorporation of carboxyl functionalized single walled carbon nanotubes (CfSWCNTs) and nylon*, Materials Science and Engineering: C, vol. 60, pp. 204-210, 2016, doi: 10.1016/j.msec.2015.11.030

[2] A.M. Schwartz, K.X. Farley, G.N. Guild, T.L. Bradbury, *Projections and Epidemiology of Revision Hip and Knee Arthroplasty in the United States to 2030,* The Journal of Arthroplasty, vol. 35, iss. 6, pp. 79-85, 2020, doi: 10.1016/j.arth.2020.02.030

[3] B. Aksakal, O.S. Yildirim, H. Gul, *Metallurgical failure analysis of various implant materials used in orthopedic applications,* Journal of Failure Analysis and Prevention, vol, 4, pp. 17–23, 2004, doi: 10.1007/s11668-996-0007-9

[4] S. Solanke, V. Gaval, S. Sanghavi, *In vitro tribological investigation and osseointegration assessment for metallic orthopedic bioimplant materials,* Materials Today: Proceedings, vol. 44, pp. 4173-4178, 2021, doi: 10.1016/j.matpr.2020.10.528

[5] K. Prasad, O. Bazaka, M. Chua, M. Rochford, L. Fedrick, J. Spoor, R. Symes, M. Tieppo, C. Collins, A. Cao, D. Markwell, K. Ostrikov, K. Bazaka, *Metallic Biomaterials: Current Challenges and Opportunities,* Materials, vol. 10, iss. 8, 2017, doi: 10.3390/ma10080884

[6] N.W. Khun, Z. Li, K.A. Khor, J. Cizek, *Higher in-flight particle velocities enhance in vitro tribological behavior of plasma sprayed hydroxyapatite coatings*, Tribology International, vol. 103, pp. 496-503, 2016, doi: 10.1016/j.triboint.2016.08.006

[7] Y. Fu, A. W. Batchelor, Y. Wang, K. A. Khor, *Fretting wear behaviours of thermal sprayed hydroxyapatite coating under unlubricated conditions*, Wear , vol. 217, iss. 1, pp. 132-139, 1998, doi: 10.1016/S0043-1648(98)00142-2

[8] M. Buciumeanu, A. Araujo, O. Carvalho, G. Miranda, J.C.M. Souza, F.S. Silva, B. Henriques, *Study of the tribocorrosion behaviour of Ti6Al4V – HA biocomposites*, Tribolology International, vol. 107, pp. 77–84, 2017, doi: 10.1016/j.triboint.2016.11.029.

[9] A.J. Rahyussalim, A.F. Marsetio, I. Saleh, T. Kurniawati, Y. Whulanza, *The Needs of Current Implant Technology in Orthopaedic Prosthesis Biomaterials Application to Reduce Prosthesis Failure Rate,* Journal of Nanomaterials, vol. 2016, pp. 1-9, 2016. doi: 10.1155/2016/5386924

[10] A.A. Zadpoor, *Current Trends in Metallic Orthopedic Biomaterials: From Additive Manufacturing to Bio-Functionalization, Infection Prevention, and Beyond*, International Journal of Molecular Sciences, vol. 19, iss. 9, 2018, doi: 10.3390/ijms19092684

[11] Y. Luo, S. Ge , Z. Jin , J. Fisher, *Effect of surface modification on surface properties and tribological behaviours of titanium alloys,* Proceedings of the Institution of Mechanical Engineers, Part J: Journal of Engineering Tribology, vol. 223, iss. 3, pp. 311–316, 2009, doi: 10.1243/13506501JET488

[12] L. Sun, *Thermal Spray Coatings on Orthopedic Devices: When and How the FDA Reviews Your Coatings*, Journal of Thermal Spray Technology, vol. 27, pp. 1280–1290, 2018, doi: 10.1007/s11666-018-0759-2

[13] L. Wang, J.C. Fang, Z.Y. Zhao, H.P. Zeng, *Application of backward propagation network for forecasting hardness and porosity of coatings by plasma spraying*, Surface and Coatings Technology, vol. 201, iss. 9-11, pp. 5085–5089, 2007, doi: 10.1016/j.surfcoat.2006.07.088

[14] H. Du, S.W. Lee, J.H. Shin, *Study on porosity of plasma-sprayed coatings by digital image analysis method,* Journal of Thermal Spray Technology, vol. 14, pp. 453-461, 2005, doi: 10.1361/105996305X76450

[15] C.S. Ramachandran, V. Balasubramanian, P.V. Ananthapadmanabhan, *On resultant properties of atmospheric plasma sprayed yttria stabilised zirconia coating deposits: designed experimental and characterisation analysis,* Surface Engineering, vol. 27, iss. 3, pp. 217–229, 2011, doi: 10.1179/1743294410Y.0000000006

[16] D. Thirumalaikumarasamya, K. Shanmugama, V. Balasubramanian, *Influences of atmospheric plasma spraying parameters on the porosity level of alumina coating on AZ31B magnesium alloy using response surface methodology Progress in Natural Science*, Materials International, vol. 22, iss. 5, pp. 468-479, 2012, doi: 10.1016/j.pnsc.2012.09.004

[17] G.L. Zhao, G.W. Wen, K. Wu, *Influence of processing parameters and heat treatment on phase composition and microstructure of plasma sprayed hydroxyapatite coatings*, Transactions of Nonferrous Metals Society of China, vol. 19, pp. 463-469, 2009, doi: 10.1016/S1003-6326(10)60090-8

[18] K.A. Gross, C.C. Berndt, H. Herman, *Amorphous phase formation in plasma-sprayed hydroxyapatite coatings,* Journal of Biomedical Materials Research, vol. 39, iss. 3, pp. 407-414, 1998, doi: 10.1002/(SICI)1097-4636(19980305)39:3<407::AIDJBM9>3.0.CO;2-N

[19] O. Sarikaya, *Effect of some parameters on microstructure and hardness of alumina coatings prepared by the air plasma spraying process,* Surface and Coatings Technology, vol. 190, iss. 2–3, pp. 388–393, 2005, doi: 10.1016/j.surfcoat.2004.02.007

[20] M.F. Hasan , J. Wang, C.C. Berndt, *Effect of Power and Stand-Off Distance on Plasma Sprayed Hydroxyapatite Coatings,* Materials and Manufacturing Processes, vol. 28, iss. 12, pp. 1279-1285, 2013, doi: 10.1080/10426914.2013.811730

[21] A. Dey, A. Sinha, K. Banerjee, A.K. Mukhopadhyay, *Tribological studies of microplasma sprayed hydroxyapatite coating at low load,* Materials Technology, vol. 29, iss. 1, pp. 35-40, 2014, doi: 10.1179/1753555713Y.0000000105

[22] S.G. Solanke , V.R. Gaval , *Tribological Studies of Different Bioimplant Materials for Orthopaedic Application,* ASM Science Journal, vol. 13, pp. 1-8, 2020, doi: 10.32802/asmscj.2020.526

[23] C.N. Elias, D.J. Fernandes , F.M. de Souza, E.S. Monteiro, R.S. de Biasi**,** *Mechanical and clinical properties of titanium and titanium-based alloys (Ti G2, Ti G4 cold worked nanostructured and Ti G5) for biomedical applications,* Journal of Materials Research and Technology, vol. 8, iss. 1, 2019, pp. 1060-1069, doi: 10.1016/j.jmrt.2018.07.016

[24] S.G. Solanke, V.R. Gaval, *Optimization of wet sliding wear parameters of Titanium grade 2 and grade 5 bioimplant materials for orthopedic application using Taguchi method,* Journal of Metals, Materials and Minerals, vol. 30, no. 3, 2020, doi: 10.14456/jmmm.2020.44

[25] C.S. Yip, K.A. Khor, N.L. Loh, P. Cheang, *Thermal spraying of Ti-6Al-4V/hydroxyapatite composites coatings: powder processing and post-spray treatment*, Journal of Materials Processing Technology, vol. 65, iss. 1-3, pp. 73-79, 1997, doi: 10.1016/0924-0136(95)02244-9

[26] ISO 13779-6, Implants for surgery Hydroxyapatite- Part 6: Powders, 2015.

[27] S.W.K. Kweh, K.A. Khor, P. Cheang, *Plasma-sprayed hydroxyapatite (HA) coatings with flame-spheroidized feedstock: microstructure and mechanical properties*, Biomaterials, vol. 21, iss. 12, pp. 1223-1234, 2000, doi: 10.1016/S0142-9612(99)00275-6

[28] P. Cheang, K.A. Khor, *Thermal spraying of hydroxyapatite (HA) coatings: Effects of powder feedstock*, Journal of Materials Processing Technology, vol. 48, issue 1-4, pp. 429-436,1995, doi: 10.1016/0924-0136(94)01679-U

[29] ISO 19227, Implants for surgery-Cleanliness of orthopedic implants-General requirements, 2018

[30] T. Kokubu, H. Kushitani , S. Sakka , T. Kitsugi, T. Yamamuro, *Solutions able to reproduce in vivo surface-structure changes in bioactive glass-ceramic*, Journal of Biomedical Material Research, vol. 24, iss. 6, pp. 721-734, 1990, doi: 10.1002/jbm.820240607

[31] M. Ipavec, A. Iglic, V.K. Iglic, K. Srakar, *Stress distribution on the hip joint articular surface during gait,* Pflügers Archiv - European Journal of Physiology, vol. 431, pp. 275-276, 1996, doi: 10.1007/BF02346375

[32] L. Neumann, K.G. Freund, K.H. Sorenson, *Long-term results of Chernley total hip replacement Review of 92 patients at 15 to 20 years*, The Journal of Bone and Joint Surgery, vol. 76, pp. 245-251, 1994, doi:10.1302/0301-620x.76b2.8113285

[33] J.G. Odhiambo, W. Li , Y.T. Zhao, C.L. Li , *Porosity and Its Significance in Plasma-Sprayed Coatings,* Coatings, vol. 9, iss. 7, 2019, doi: 10.3390/coatings9070460

[34] ISO 13779-2, Implants for surgery – Hydroxyapatite - Part 2: Thermally sprayed coatings of hydroxyapatite, 2018.

[35] ISO 13779-4, Implants for surgery - Hydroxyapatite - Part 4: Determination of coating adhesion strength, 2018.

[36] Y. Lu, S.T. Li, R.F. Zhu, M.S. Li , *Further studies on the effect of stand-off distance on characteristics of plasma sprayed hydroxyapatite coating,* Surface and Coatings Technology, vol. 157, iss. 2, pp. 221–225. 2002, doi: 10.1016/S0257-8972(02)00166-4

[37] C. Shilpa, K. Mahesha, A. Dey, K.B. Sachidananda, *Effect of stand-off distance (SOD) on damping properties of atmospheric plasma sprayed alumina-zirconia ceramic coatings,* Surface Engineering, vol. 37, iss. 5, 2020, doi: 10.1080/02670844.2020.1780674

[38] J. Geringer, B. Forest, P. Combrade, *Wear analysis of materials used as orthopaedic implants,* Wear, vol. 261, iss. 9, pp. 971-979, 2006, doi: 10.1016/j.wear.2006.03.022

[39] P. Brodin, *New approaches to the study of immune responses in humans,* Human Genetics, vol. 139, pp. 795–799, 2020, doi: 10.1007/s00439-020-02129-3

[40] R. Singh, D. Pantarotto, L. Lacerda, G. Pastorin, C. Klumpp, M. Prato, A. Bianco, K. Kostarelos, *Tissue biodistribution and blood clearance rates of intravenously administered carbon nanotube radiotracers*, Proceedings of the National Academy of Sciences of the United States of America, vol. 103, iss. 9, pp. 3357-3362, 2006, doi: 10.1073/pnas.0509009103

[41] V.E. Kagan, N.V. Konduru, W. Feng, B.L. Allen,J. Conroy,Y. Volkov, I.I. Vlasova, N.A. Belikova, N. Yanamala, A. Kapralov,Y.Y. Tyurina, J. Shi, E.R. Kisin, A.R. Murray, J. Franks., D. Stolz,P. Gou, J. Klein-Seetharaman, B. Fadeel, A. Star, A.A. Shvedova, *Carbon nanotubes degraded by neutrophil myeloperoxidase induce less pulmonary inflammation,* Nature Nanotech, vol. 5, pp. 354–359, 2010, doi: 10.1038/nnano.2010.44

[42] K. Kostarelos, *Carbon nanotubes fibrillar pharmacology,* Nature Materials, vol. 9, pp. 793-795, 2010 , doi: 10.1038/nmat2871

[43] L. Pawlowski, *The Science and Engineering of Thermal Spray Coatings,* New York: Wiley, 1995

[44] S. Kaur, K. Ghadirinejad, R.H. Oskouei, *An Overview on the Tribological Performance of Titanium Alloys with Surface Modifications for Biomedical Applications*, Lubricants, vol. 7, iss. 8, 2019, doi: 10.3390/lubricants7080065

[45] A. Dey, A.K. Mukhopadhyay, *In-vitro dissolution, microstructural and mechanical characterizations of microplasma sprayed hydroxyapatite coating*, International Journal of Applied Ceramic Technology, vol. 11, iss. 1, 2014, doi: 10.1111/ijac.12057

[46] Y. Fu, A.W. Batchelor, Y. Wang, K.A. Khor, *Fretting wear behaviours of thermal sprayed hydroxyapatite coating lubricated with bovine albumin,* Wear, vol. 230, iss. 1, pp. 98-102, 1999, doi: 10.1016/S0043-1648(98)00340-8

[47] F. Živić , N. Grujović , S. Mitrović , D. Adamović, V. Petrović , A. Radovanović , S. Đurić , N. Palića, *Friction and Adhesion in Porous Biomaterial Structure,* Tribology in Industry, vol. 38, iss. 3, pp. 361-370, 2016.

[48] F.Z. Derradji , M. Labaïz , M. Bououdina , A. Ourdjini, A. Montagne, A. Iost, *Porous plasma sprayed bioceramic (Ca10 (PO4).6(OH)2) coated Ti6Al4V: morphological, adhesion and tribological studies*, Materials Research Express, vol. 6, no. 9, 2019, doi: 10.1088/2053-1591/ab2a1c

[49] L.L. Badita, G. Gheorghe, L. Capitanu, *Investigation of Nanostructured Thin Films Adhesion used to Improve Tribological Characteristics of Hip Prostheses*, Tribology in Industry, vol. 36, No. 4, pp. 437-450, 2014.

[50] A. Fomin, M. Fomina, V. Koshuro, I. Rodionov, A. Zakharevich, A. Skaptsov, *Structure and mechanical properties of hydroxyapatite coatings produced on titanium using plasma spraying with induction preheating*, Ceramics International, vol. 43, iss. 14, pp. 11189-11196, 2017, doi:10.1016/J.CERAMINT.2017.05.168

[51] A. Dey, A.K. Mukhopadhyay, *Nanoindentation Study of Phase-pure Highly Crystalline Hydroxyapatite Coatings Deposited by Microplasma Spraying*, Open Biomed Eng Journal, vol. 9, pp. 65-74, 2015, doi: 10.2174/1874120701509010065

[52] R. Sharifi, D. Almasi, I.B. Sudin, M. Kadir, L. Jamshidy, S.M. Amiri, H.R. Mozaffari, M. Sadeghi, F. Roozbahani, N. Iqbal, *Enhancement of the Mechanical Properties of Hydroxyapatite/Sulphonated Poly Ether Ether Ketone Treated Layer for Orthopaedic and Dental Implant Application*, International Journal of Biomaterials, vol. 2018, pp. 1-9, 2018, doi: 10.1155/2018/9607195

[53] Q. Zhao, D. He, L. Zhao, X. Li, *In-vitro Study of Microplasma Sprayed Hydroxyapatite Coatings in Hanks Balanced Salt Solution*, Materials and Manufacturing Process, vol. 26, iss. 2, pp. 175–180, 2011,doi: 10.1080/10426914.2010.498071

[54] C.E. Mancini, C.C Berndt, L. Sun, A. Kucuk, *Porosity Determinations in Thermally Sprayed Hydroxyapatite Coatings*, Journal of Materials Sciience, vol. 36, iss. 16, pp. 3891–3896, 2001, doi: 10.1023/A:1017905818479